

Image formation and contrast inversion in noncontact atomic force microscopy imaging of oxidized Cu(110) surfaces

J. Bamidele,¹ Y. Kinoshita,² R. Turanský,³ S. H. Lee,² Y. Naitoh,² Y. J. Li,² Y. Sugawara,² I. Štich,³ and L. Kantorovich^{1,*}

¹*Department of Physics, King's College London, The Strand, London WC2R 2LS, UK*

²*Department of Applied Physics, Osaka University, 2-1 Yamada-oka, Suita, Osaka 565-0871, Japan*

³*Center for Computational Materials Science, Institute of Physics, Slovak Academy of Sciences, 84511 Bratislava, Slovakia*

(Received 9 April 2014; published 10 July 2014)

Joint experimental and theoretical investigation of image formation in noncontact atomic force microscopy (NC-AFM) of the $c(6 \times 2)$ and $p(2 \times 1)$ phases of the Cu(110):O surface is presented. We proposed previously that the $c(6 \times 2)$ reconstruction of the Cu(110):O surface may serve as a reference system allowing chemical identification of the tip apex atom during the course of NC-AFM experiments. The identification is possible due to the fact that two most likely possible contrasts that could be observed after intermittent contacts of the tip with the surface were found which can be attributed to the tip being either terminated by Cu or O atoms. In this paper the idea of exploiting the Cu(110):O surface in NC-AFM studies is further developed. Specifically, (i) we show that there must be an image contrast inversion when the $c(6 \times 2)$ surface reconstruction is scanned depending on the tip-surface distance: at the usual imaging conditions, at tip-sample distances of 2–5 Å, the previously reported contrast is observed; however, an opposite contrast is observed for larger separations with one of the two tip terminations. (ii) We study in detail also the image contrast formation of the $p(2 \times 1)$ surface, which is another common surface reconstruction, and show that tip identification for it is not possible. (iii) Finally, we discuss here possible effects of the actual tip atomic structure on the NC-AFM image. In particular, we show that the O-terminated tip will remain such even after picking up a Cu atom from the surface, experimentally a frequently observed process. Hence this type of the tip modification would only affect secondary features in the image.

DOI: [10.1103/PhysRevB.90.035410](https://doi.org/10.1103/PhysRevB.90.035410)

PACS number(s): 68.37.Ps, 81.16.Ta, 68.35.B–

I. INTRODUCTION

Noncontact atomic force microscopy (NC-AFM), based on measuring forces between the surface and an atomically sharp probe, has proven to be an indispensable tool in the modern toolkit of experimental surface probe methods as it allows obtaining, in many cases, atomic resolution of crystal surfaces, both conducting and insulating [1,2]. However, similarly to another popular technique of scanning tunneling microscopy [3,4], which is limited to conducting surfaces, interpretation of the obtained NC-AFM images is often difficult as these are affected by the tip structure which is usually unknown.

It was recently proposed [5] that the Cu(110):O- $c(6 \times 2)$ surface may serve as a convenient reference system allowing tip apex identification during the scan, even after the tip change. The surface in question, Fig. 1(b), formed at high oxygen exposure, consists of added rows (ARs) of alternating Cu and O atoms placed on top of the Cu(110) bulk termination and running in the [001] direction; the rows are “connected” by additional Cu atoms (called “super” Cu atoms) sitting in the missing rows which bind the opposite O atoms of the adjacent Cu-O rows. The super Cu atoms pull the two oxygen atoms (called “high O”) towards them and slightly up thereby forming a distinctive CuO₂ “molecule.” The other surface termination, the $p(2 \times 1)$, Fig. 1(a), corresponding to a lower O exposure, also consists of ARs of alternating Cu and O atoms running in the [001] direction, similarly to the $c(6 \times 2)$, but the low O exposure phase lacks the distinctive super Cu atoms. As a

result these two phases yield dramatically different NC-AFM images, and, as shown below, only the former is appropriate for chemical identification of the tip apex atom.

Experimental images of the $c(6 \times 2)$ phase, when imaged with a tip produced by indenting into Cu-O clusters frequently found on the surface, appear with only two main contrasts: either as a single- or a double-spot feature. The corresponding theoretical analysis, based on density functional theory (DFT) calculations, revealed without doubt that the single-spot contrast is due to an O-terminated tip (type I), while the double-spot features appear when the tip is Cu terminated (type II). Although only two main features were observed, secondary features were also found to exist in the images which change depending on the imaging conditions. These were attributed to the actual tip “atomic structure” which, unlike chemical tip termination or identity, is impossible to control. In other words, although the tip apex atom remained either Cu or O (leading to the main contrast), other tip atoms may adopt a multitude of different chemical and geometrical (structural) conformations leading to the observed variations of the secondary features in the images. We call these chemical and structural factors “tip structure.” In addition, depending on the experimental frequency shift, different contrasts on the $c(6 \times 2)$ have been observed with images of Cu atoms, O atoms, or “high O - super Cu - high O” chains as bright [5,6] features which arise due to different tip-surface interaction regimes, while only a single type of contrast was observed on the $p(2 \times 1)$ phase.

Our previous paper [5] was focused on the tip and its chemical identity and our main objective was to explain the primary features in the experimental image of the $c(6 \times 2)$ phase only under typical imaging conditions. Contrary to the experimental observations of that phase, the $p(2 \times 1)$ phase

*lev.kantorovitch@kcl.ac.uk

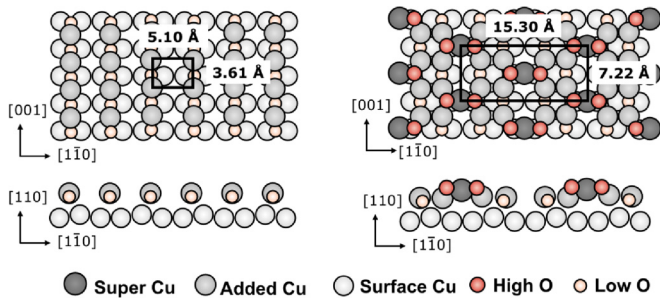


FIG. 1. (Color online) Ball model of top and side views of the $p(2 \times 1)$ phase (left), where light red, gray, and light gray balls depict low O, added Cu, and bulk Cu atoms, respectively, and of the $c(6 \times 2)$ phase (right), where additionally dark gray and red balls depict the super Cu and high O atoms.

appears to give only one type of image, alternating bright and dark spots, irrespective of the chemical tip termination, and, hence, appears to be insensitive to the chemical tip identity. Therefore, in this paper we consider in detail the $p(2 \times 1)$ phase and clarify the different contrasts observed and unaccounted for on the $c(6 \times 2)$ phase. With all the experimental subtleties in mind, we address here the following issues: (i) dependence of the observed contrast on the $c(6 \times 2)$ surface on the tip-surface separation; (ii) effect of the tip structure and its consequences for the secondary features in the NC-AFM image on both phases; and, (iii) image formation on the $p(2 \times 1)$ surface and why is it that this surface termination is not appropriate for the chemical identification of the tip apex atom. These findings along with Ref. [5] provide a complete understanding of the images of the oxidized Cu(110) surfaces and provide a basis for understanding also of the atomic manipulation on them with NC-AFM [7].

In the next section we shall briefly describe our experimental and theoretical methods; the main results are reported in Sec. III. The paper concludes with the summary of our main results and conclusions.

II. METHODS

Since our experimental and theoretical methods are essentially the same as in our previous study [5], only a very brief account will be given here. All experiments were carried out under ultrahigh-vacuum conditions at 78 K by a home-built NC-AFM using the frequency-modulation technique [8] and low-resistivity (0.01–0.025 Ω cm) n-doped commercial silicon cantilevers (Nanoworld, Switzerland). The oscillation amplitude was kept constant at between 5.3 and 8.3 nm. The cantilevers typically had a Q factor of 1.5×10^5 , spring constant of 40 N/m, and resonance frequencies of 150 kHz. To prepare the Cu(110):O surface, the sample was first cleaned by Ar sputtering, annealed, and then exposed to 2000 L of oxygen at 300 °C. The tip apex was cleaned by Ar ion sputtering (650 eV) *in situ*. Both the cantilever and the sample were always electrically grounded.

Theoretical calculations were performed using DFT and the VASP code [9,10], based on a plane wave basis set and projector augmented wave potentials [10,11]. The effect of exchange and correlation was described using the gradient-corrected

Perdew-Burke-Ernzerhof (PBE) functional [12]. Forces on atoms were converged to 0.01 eV/Å. To model the tip, we used a relatively stiff Cu tetrahedron employing either an O or Cu atom at its asperity; see Fig. 3. In addition, as described below in detail, four more tip models were used in which an additional Cu/O atom was added to the tip at two positions to model a possible tip change by accepting an extra Cu/O atom from the surface during the scan (vertical manipulation). In all cases, only the lowest four (five) atoms of the tip were allowed to relax upon interaction with the surface.

Frequency shift curves were calculated in the usual way by assuming a spherical macroscopic tip above the tip cluster described above; the macroscopic tip provided an additional van der Waals background force between the tip and surface.

III. RESULTS

We now study the $c(6 \times 2)$, Sec. III A, and $p(2 \times 1)$, Sec. III B, surfaces in terms of factors affecting the NC-AFM image formation, such as different chemical tip termination and frequency shift, which affect the primary features in the image. The effect of the tip structure, which affects the secondary image features, is studied in Sec. III C.

A. The $c(6 \times 2)$ surface

Our experimental and theoretical results for two-dimensional maps of the frequency shift, Δf , measured along the $[1\bar{1}0]$ direction and in the plane perpendicular to the oxidized Cu(110) surface, are shown in Fig. 2. This line goes across the “high O - super Cu - high O” chain, see Fig. 1, and hence contains most of the features of the surface including a hollow site. These results correspond to the dependence of the frequency shift on the tip height along the indicated line. The experimental results acquired with the O-terminated (type I) tip, Fig. 2(a), indicate that at smaller $|\Delta f|$ values the tip images Cu atoms as brightest, but as the tip-surface distance reduces both the super Cu and high O atoms are imaged as bright. In either case a clearly single feature is seen on the place of the chain (or the CuO₂ “molecule”). This result may also give a valid explanation of the different contrasts observed for the type I tip in [5], where in Fig. 6(c) the super Cu atoms appear circular while in Fig. 7(d) they appear elliptical with some subsurface features also observed. Similarly, they also help in explaining the three similar but different contrasts reported by Kishimoto *et al.* [6], as at different Δf values either just the Cu atoms appear as brightest at smaller $|\Delta f|$ values, or both the Cu atoms and the O can be imaged as a single feature at larger $|\Delta f|$ values.

The experimental results corresponding to the Cu-terminated (type II) tip, Fig. 2(c), show that at small $|\Delta f|$ values the “high O - super Cu - high O” chain is imaged as bright, with the super Cu atom as brightest. As the tip-surface interaction increases, the super Cu and high O atoms in the chain are first imaged as equally bright, but then, as the tip-surface interaction becomes stronger (higher $|\Delta f|$ values), the super Cu atoms are imaged only as depressions, while the high O atoms are imaged clearly as the brightest features leading to double bright spots to be observed in places of the CuO₂ “molecules.” Similar trends are also seen

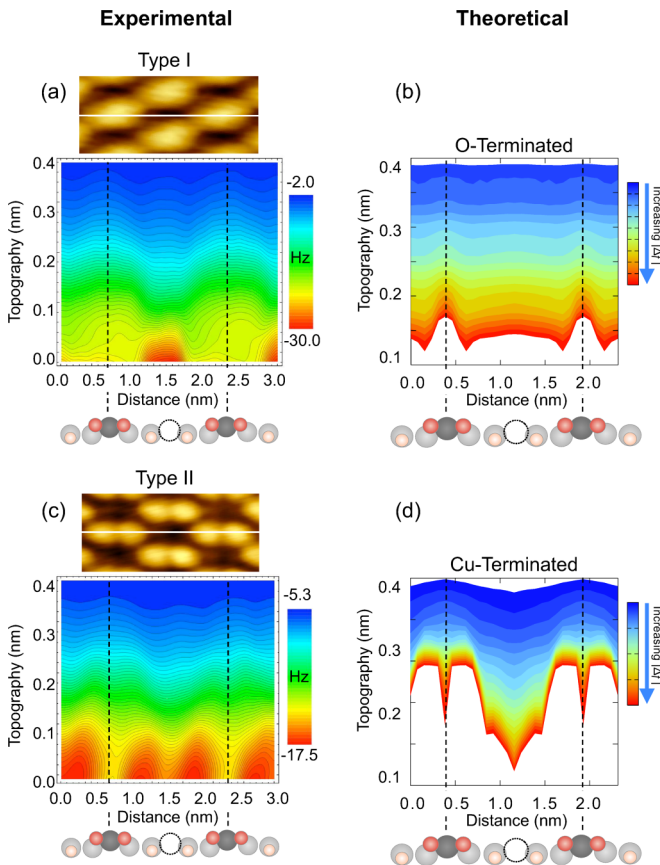


FIG. 2. (Color online) Experimental [(a), (c)] and theoretical [(b), (d)] constant frequency shift NC-AFM topography scan lines of the $\text{Cu}(110)\text{-}c(6 \times 2)$ surface corresponding to the O- [(a) and (b)] and Cu- [(c) and (d)] terminated tips, respectively, plotted for a wide range of Δf values. The corresponding topography images were obtained at oscillation amplitudes A and frequency shifts Δf of (a) $A = 8.3$ nm and $\Delta f = -17.5$ Hz and (c) $A = 5.3$ nm and $\Delta f = -8.3$ Hz, respectively. These are shown above both experimental scan line images in (a) and (c), where the white lines indicate the region where the tip scans. A cartoon depicting the surface from a side view is also shown below each plot.

in the experimental topography images in Fig. 2(c). Therefore, experimentally we observe an *inversion* of contrast at closer approach as compared to the weaker interaction regime.

These experimental findings, especially the primary image features, are corroborated also by theoretical modeling despite use of fairly simple and stiff tip models. In particular, for the O-terminated tip (type I) we find in agreement with experiments that this tip termination images primarily the super Cu atoms. However, the trend that as $|\Delta f|$ increases the super Cu atoms will appear much brighter than both the high O atoms and the hollow sites is not born out in experiments, when at smaller tip-surface distances (larger $|\Delta f|$) the entire CuO_2 “molecules” are imaged appearing equally bright, while the hollow sites get darker. For the Cu-terminated (type II) tip, our model correctly describes the contrast inversion when imaging the $c(6 \times 2)$ surface at different $|\Delta f|$ values. Such an agreement between theory and experiment for a wide range of the $|\Delta f|$ values presented here, in spite of the very simple tip models, gives an

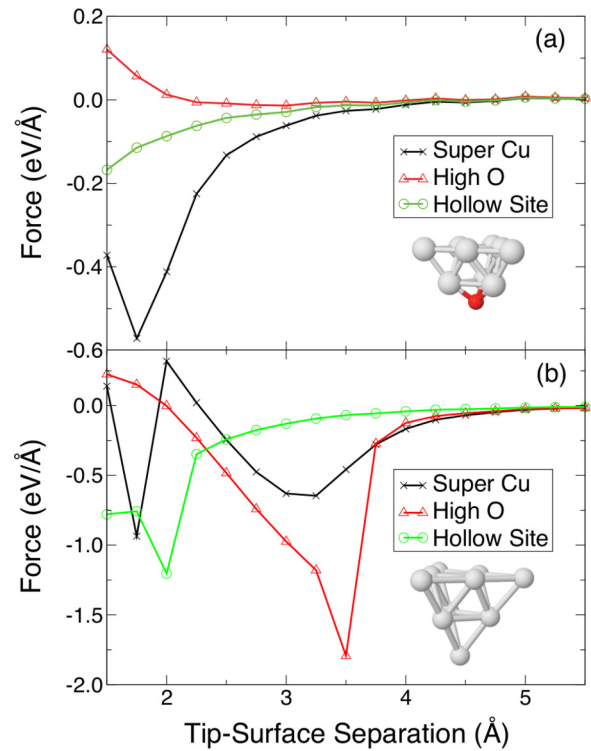


FIG. 3. (Color online) Calculated short-ranged force-distance curves for the O-terminated (a) and Cu-terminated (b) tips positioned above the super Cu (black), high O (red), and hollow site (green) of the oxidized $\text{Cu}(110)\text{-}c(6 \times 2)$ surface. The tip heights shown correspond to the distance between the apex tip atom and the super Cu atom of the surface *prior* to geometry relaxation. Cartoons depicting the tip models are also shown in each case. The light gray and red balls correspond to Cu and O atoms, respectively.

additional strong support for the tip characterization proposed previously [5].

To understand better the change of the contrast discussed above, the calculated force-distance curves are shown in Fig. 3 for the two tip models. The case of the O-terminated tip interaction with the super Cu atom is the strongest over the whole range of tip-surface distances, and this corresponds to the super Cu atoms imaged brightest for all values of the frequency shift. In the case of the Cu-terminated tip, however, the situation is very different. At large heights interaction with the surface above super Cu atoms is slightly stronger than when the tip is positioned above the high O atoms; however, for the tip-surface distance of approximately 3.8 Å and below the interaction is the strongest above the high O atoms, and this situation continues until well into the repulsive regime.

Hence, for a wide range of typical experimental tip heights (around $2.5\text{--}3$ Å of tip-surface distance as defined here) Cu-terminated tips image O atoms and O-terminated tips image Cu atoms. At the same time, at relatively large tip-surface distances a different contrast is observed for the Cu-terminated tip.

Summarizing our findings, from the experimental point of view the conclusion on the tip termination identification made previously [5] has to be modified as follows: (i) If the super Cu atoms are clearly imaged at small $|\Delta f|$ values, where they

appear as single circular bright spots, but then at larger $|\Delta f|$ values both the super Cu and high O atoms are imaged resulting in the spot being deformed into an elliptical one, then this situation corresponds to the O-terminated tip. (ii) If the Cu atoms are imaged at small $|\Delta f|$ values, where they appear as a single circular bright spot, but then at larger $|\Delta f|$ values the O atoms appear as bright and the Cu atoms appear as dark, leading to appearance of two bright spots instead, then this corresponds to the Cu-terminated tip. It is clear that the key in the tip identification still remains the fact of whether double bright features are seen or not at the frequency shifts corresponding to the strong tip-surface interaction when the contrast is strong. Experimentally this fact can be established by gradually increasing the frequency shift during scan.

B. The $p(2 \times 1)$ surface

In Ref. [5] we reported on the same experimental images that the $c(6 \times 2)$ phase may coexist with the $p(2 \times 1)$ one. In the latter the arrangement of the Cu-O rows running along the [001] direction is different from that in the $c(6 \times 2)$ phase, and the $p(2 \times 1)$ phase does not have extra Cu atoms on top of the rows. It is seen in the images reported previously in [5] that while the contrast of the $c(6 \times 2)$ phase does change with the tip termination, the image of the coexisting $p(2 \times 1)$ phase stays the same, consisting of a periodic arrangement of identical bright spots. By reporting here on the theoretical modeling of this surface termination, we would like to answer two questions: (i) which species (Cu or O) in the rows are shown in the images of the $p(2 \times 1)$ phase when scanning with either of the tip terminations, and (ii) whether there is a contrast inversion when going from small to large frequency shift values when scanning this particular phase. This will also act as a check of the validity of our model, since to accurately simulate a scan of the $c(6 \times 2)$ surface, our model must also accurately simulate a scan of the $p(2 \times 1)$ surface.

From our calculations performed on the $c(6 \times 2)$ phase we know that the contrast is established due to interaction between Cu and O atoms of the tip and surface. Then, since the periodicities of Cu and O atoms along the rows running along the [001] direction of the $p(2 \times 1)$ surface are identical, we expect that identification of the chemical species terminating the tip by scanning this surface is impossible. And indeed, experimental constant frequency shift images shown in Figs. 4(a) and 4(d) with the two tips show the two images looking almost exactly the same demonstrating an identical arrangement of bright spots with the same periodicity, as expected. This is confirmed in detail by scan lines along the red line indicated on both images which are shown in panels (b) and (e); they show that for both tips only one species is imaged, measured with a periodicity of ≈ 0.31 nm. Note that the tip model is unequivocally determined in each case by the image of an island of the $c(6 \times 2)$ phase existing nearby and imaged at the same time (not shown; see, e.g., Figs. 3 and 4 in [5]).

To confirm the experimental findings, we have also performed theoretical simulations of a scan line on the $p(2 \times 1)$ surface for a range of frequency shift values, taken along the row of alternating Cu and O atoms in the [001] direction also corresponding to the red lines on the experimental images (a) and (d) in Fig. 4. Theoretical calculations predict a periodicity

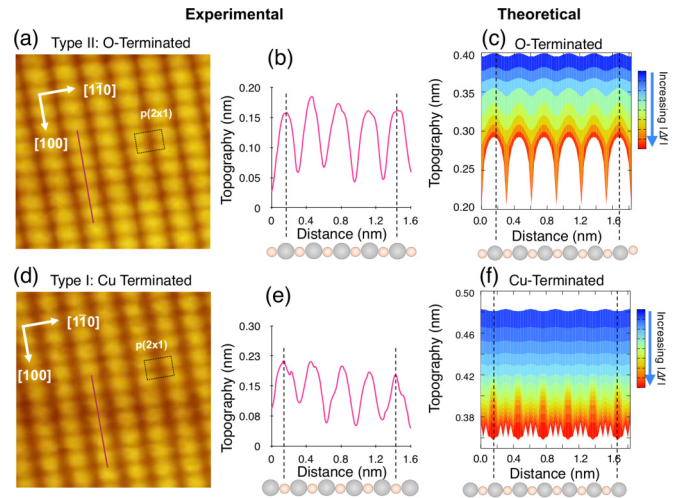


FIG. 4. (Color online) Experimental NC-AFM topography images [(a), (d)], scan lines [(b), (e)], and theoretical constant frequency shift topography scan lines [(c), (f)] of the Cu(110)- $p(2 \times 1)$ surface corresponding to the O- [(a)–(c)] and Cu- [(d)–(f)] terminated tips. Imaging conditions: (a), (b) $A = 6.7$ nm, frequency shift $\Delta f = -18.7$ Hz; (d), (e) $A = 6.7$ nm, frequency shift $\Delta f = -16$ Hz. The theoretical scan lines are shown for a range of frequency shift $|\Delta f|$ values. The red line on the experimental topography images indicates the region where the line scans shown in (b), (e) were taken. A cartoon depicting the surface from a side view is also shown below each plot, color coded as in Fig. 2.

of ≈ 0.30 nm between bright spots, in good agreement with experiment. We also see that each tip images only a single species for any frequency shift value. At the same time, we observe that the O-terminated tip images exclusively Cu atoms across all $|\Delta f|$ values, while the Cu-terminated tip does indeed produce a contrast inversion as $|\Delta f|$ increases: imaging the O atoms as brightest at small $|\Delta f|$ values, and then imaging Cu atoms as brightest at the larger $|\Delta f|$ values. We see that, similarly to the case of the $c(6 \times 2)$ phase, the contrast inversion is expected for the $p(2 \times 1)$ surface with the Cu-terminated tip as well.

Although we expect subtle differences between experiment and theory as the latter is using very simple tip models, for typical imaging Δf values we observe good agreement between the two, as both predict that only either Cu or O atoms are imaged, and that the imaged species will be different for the Cu- and O-terminated tips. This shows that our model is indeed valid for typical imaging Δf values, and also shows that experimental characterization of the tip chemical identity is impossible when scanning the $p(2 \times 1)$ surface. Considering wider range of frequency shifts, Fig. 4, the tip chemical identity when scanning the $p(2 \times 1)$ surface may also be possible, at least in principle, although perhaps not very practical, by probing the distance dependence of the contrast.

C. Effect of tip structure and secondary features

The discussion so far has been based on our idealized tip models. However we cannot be certain of the actual structure of the real tip beyond the chemical identity of the tip apex, and hence we cannot completely rule out that the observed

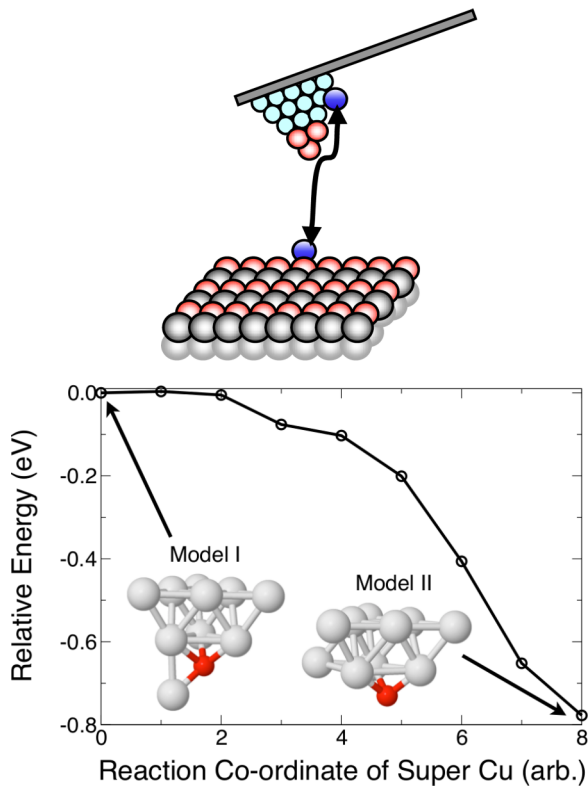


FIG. 5. (Color online) Upper panel: Schematic model of a Cu atom deposition/extraction onto/from $p(2 \times 1)$ surface without tip apex modification. Lower panel: The NEB calculated minimum energy profile for the adsorbed Cu atom to diffuse from its position next to the O apex atom (the initial structure, the tip model I) further up the tip structure to the final position (the tip model II). Inset are models of the two tip models I (left) and II (right) where an extra Cu atom is added either at the bottom of the tip next to the apex O atom, or on the side of the tip higher up. The color code is the same as in Fig. 3.

features may be related to more complex tip termination; in particular, secondary atoms in the tip (atoms other than the terminating atom) may substantially change the observed features [13,14]. Experimentally, a very easy deposition of Cu atoms from an O-terminated tip onto the oxidized surface was observed [5,7], with the reverse Cu-atom extraction being also possible albeit with much lower probability [7]; see the schematic drawing in Fig. 5 (top panel). Since the contrast of the surface did not change during these observations, one has to assume that the tip remained O terminated. Therefore, such additional Cu atoms must come from the parts of the tip other than the apex and hence may modify the nearby atomic tip structure. We have indeed identified secondary effects in our images of both $c(6 \times 2)$ and $p(2 \times 1)$ phases, with the effect being much more pronounced in the former case; see, for instance, Figs. 3 and 4 in [5]. There one may argue that the differences in the images of both phases are caused by change in the tip structure, as opposed to chemical tip termination. To discuss these possibilities, alternative tip models have also been considered.

Four such alternative tip models were considered: (I) an O-terminated tip with a Cu atom adsorbed at the bottom near the

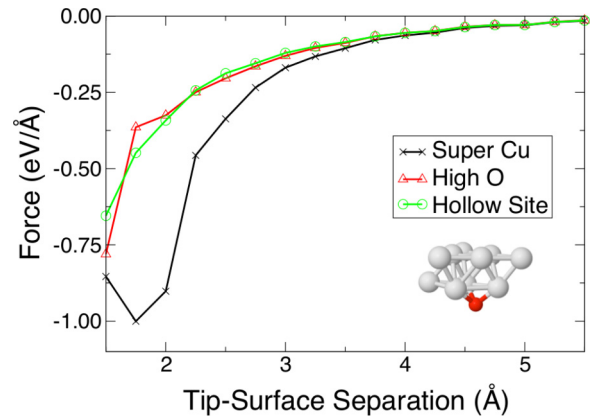


FIG. 6. (Color online) Calculated short-ranged force-distance curves above the same three lattice sites as in Fig. 3 for the tip model II formed by adsorbing an extra Cu atom on what was originally the O-terminated tip.

O apex atom; (II) an O-terminated tip with a Cu atom adsorbed on the side above the apex O atom; (III) a Cu-terminated tip with an O atom adsorbed at the bottom; (IV) a Cu-terminated tip with an O atom adsorbed on the side. These models were inspired by a realistic possibility for the tip to pick up/deposit either O or Cu atom up from the surface during scanning [7].

Models I and II appeared to be stable when relaxed away from the surface; their relaxed geometries are shown as insets in Fig. 5 (bottom panel). Model II appeared to be by 0.8 eV more stable than model I. To investigate the stability of model I, we studied the diffusion of the extra Cu atom on the tip. Using the nudged elastic band (NEB) method [15,16], we considered a possible diffusion path of the extra Cu atom between models I and II. The minimum energy profile between the initial I and final II structures is shown in Fig. 5. We find that there is practically no barrier for diffusion for the Cu atom to form model II from model I. This means that model I is internally unstable in the sense that small thermal energy would be sufficient for it to be transformed into the much more stable model II.

We have also performed studies of models III and IV. However, the model III tip was found to transform into a tip very similar to model I upon interaction with the surface. Similarly the model IV tip relaxed into model II upon interaction with the surface. Therefore, these two models will not be discussed further.

Hence, it is sufficient to consider in more detail model II only. The calculated force-distance curves for this model on the $c(6 \times 2)$ phase above the same lattice sites as before are shown in Fig. 6. One can see that the interaction is the strongest above the super Cu atom; i.e., the contrast in the image with this tip would be the same as with the original O-terminated tip. This is to be expected since both tips possess the same apex atom which is the closest to the surface. At the same time, the secondary features in the image obtained with this tip would be different than obtained using the original tip. This follows from the comparison of the force curves obtained above the hollow and high O sites in the two cases; compare Figs. 3(a) and 6: if in the case of the original tip the interaction above the hollow site is stronger than above the high O, the modified

tip demonstrates the two interactions being almost the same; in fact, between 2.3 and 3.5 Å the force above the high O is slightly stronger.

Therefore, we find that the tip structure may not necessarily change the main contrast, although secondary features may be affected. Of course, to a large extent the validity of this conclusion depends on the actual structure of the tip which may be quite different from the ones considered here. And indeed many cases of the change of contrast due to atoms picked up by the tip during the scan have been reported previously [5]. However, it follows from our calculations and experimental observations that there *are* tips and tip models which do not change the *main* contrast even after picking up/depositing an atom from/to the surface; only secondary features in the image change.

IV. SUMMARY AND CONCLUSION

We presented detailed joint experimental and theoretical scan line results for both Cu(110):O surface terminations, the $c(6 \times 2)$ and the $p(2 \times 1)$, obtained in a wide range of frequency shift values. For the $c(6 \times 2)$ phase we observed that different contrasts can be obtained: the tips can image either Cu atoms, O atoms, or the “high O - super Cu - high O” chains as brightest. We then used these results to explain the different contrasts observed in [5,6] when imaging the Cu atoms (circular and elliptical shapes as well as subsurface features) as being due to measurements taken by an O-terminated tip at different tip-surface interaction regimes. We also show that in each case, the Cu atoms are still imaged as brightest.

We then went on to show why tip identification by scanning the clean $p(2 \times 1)$ surface is not possible. This is because this particular surface has identical arrangement of the Cu and O atoms. What makes the $c(6 \times 2)$ surface special is the presence and special arrangement of super Cu atoms which pull in the nearest O atoms which consequently results in the formation of the CuO₂ “molecules” that are actually imaged. This makes this particular surface suitable for chemical tip identification. As was suggested in [5], other surfaces which have similar features may appear to be also good candidates for that purpose.

We have also made an interesting observation of the contrast inversion when scanning either the $c(6 \times 2)$ or $p(2 \times 1)$ surface with the Cu-terminated tip. This finding also helps to explain the different contrasts that may be obtained with this type of the tip (e.g., circular vs elliptical features). In fact, contrast inversions have been reported several times previously, particularly on the Si(111) [17–19] and TiO₂ [20,21] surfaces, as well as on some others [22–25]; recently this has also been observed on the clean (111) surfaces of Cu with Cu tips [26] and Cu, Pt, and Ir with Pt and Ir tips [27]. In most cases this effect has been observed for the

tip positioned on top of atoms and above hollow sites, and was typically during imaging in either the attractive or repulsive regime. However, in our case the inversion is observed for the tip positioned on top of two atoms of different species. Furthermore, it appears to only occur in our case for tips with Cu atom asperities.

We believe that this behavior can be explained by simple arguments based on the Cu-Cu and Cu-O bond lengths and their strengths. The Cu-Cu bond length is larger than that of Cu-O (2.22 Å [28] and 1.73 Å [29], respectively); thus one would expect the Cu-terminated tip to interact more strongly with surface Cu atoms at larger tip-surface separations, imaging the Cu atoms as highest (brightest). However the Cu-Cu bond strength is weaker; therefore as the tip-surface separations decreases, often before the repulsive regime is even reached, the Cu-terminated tip starts interacting more strongly with the surface O atoms on both sides of the super Cu atom, thus imaging them as the highest (brightest). With the O-terminated tip, the interaction of the apex O atom with the super Cu atom determines the imaging contrast at all tip-surface distances.

Additionally we investigated other tip models which may be relevant because of atoms jumping between the surface and the tip during the scan [5,7]. These additional atoms result in change of the tip structure which may cause to change primary or secondary features in the experimental images. We find that some tip models are unstable because they would restructure either upon interaction with the surface or due to thermal activation; in some other cases, such as an O-terminated tip with an extra Cu atom added to it, the tip is stabilized without changing its chemical identity; as a result, the main contrast of the surface during the scan is not affected; only secondary features in the image may change.

The general result is that both O- and Cu-terminated tips image surface Cu atoms as brightest at small $|\Delta f|$. Based on our results, to identify the tip apex, i.e., to enforce/determine the tip chemical termination, may require simply to scan the surface at a relatively large $|\Delta f|$ values, or failing that, to crash the tip into the surface and scan again in order to eliminate ambiguity.

ACKNOWLEDGMENTS

This work is supported by a Grant-in-Aid for Scientific Research of Japan, by APVV (APVV-0207-11) and VEGA (2/0007/12), and by the Engineering and Physical Sciences Research Council (EPSRC). J.B. in particular thanks EPSRC for studentship funding. We also acknowledge the support of King’s College London’s HPC Facility managed by Dr. Alessio Comisso, the Material Chemistry consortium for the computer time allocation on the HECToR UK National Facility, and the Computing Centre of the Slovak Academy of Sciences for use of the supercomputing infrastructure funded by the ERDF, Projects No. ITMS 26230120002 and No. 26210120002.

[1] F. J. Giessibl, *Rev. Mod. Phys.* **75**, 949 (2003).
 [2] S. P. Jarvis, H. Yamada, S. I. Yamamoto, H. Tokumoto, and J. B. Pethica, *Nature (London)* **384**, 247 (1996).

[3] G. Binnig, H. Rohrer, C. Gerber, and E. Weibel, *Phys. Rev. Lett.* **50**, 120 (1983).
 [4] D. Eigler and E. K. Schweizer, *Nature (London)* **344**, 524 (1990).

- [5] J. Bamidele, Y. Kinoshita, R. Turanský, S. H. Lee, Y. Naitoh, Y. J. Li, Y. Sugawara, I. Štich, and L. Kantorovich, *Phys. Rev. B* **86**, 155422 (2012).
- [6] S. Kishimoto, M. Kageshima, Y. Naitoh, Y. J. Li, and Y. Sugawara, *Surf. Sci.* **602**, 2175 (2008).
- [7] J. Bamidele, S. H. Lee, Y. Kinoshita, R. Turanský, Y. Naitoh, Y. J. Li, Y. Sugawara, I. Štich, and L. Kantorovich, *Nat. Commun.* (to be published, 2014).
- [8] T. Albrecht, P. Grütter, D. Horne, and D. Rugar, *J. Appl. Phys.* **69**, 668 (1991).
- [9] G. Kresse and J. Furthmüller, *Phys. Rev. B* **54**, 11169 (1996).
- [10] G. Kresse and J. Furthmüller, *Comput. Mater. Sci.* **6**, 15 (1996).
- [11] P. E. Blöchl, *Phys. Rev. B* **50**, 17953 (1994).
- [12] J. P. Perdew, K. Burke, and M. Ernzerhof, *Phys. Rev. Lett.* **77**, 3865 (1996).
- [13] M. A. V. de la Cerda, J. Abad, A. Madgavkar, D. Martrou, and S. Gauthier, *Nanotechnology* **19**, 045503 (2008).
- [14] R. Bechstein, C. González, R. P. J. Schütte, P. Jelínek, and A. Kühnle, *Nanotechnology* **20**, 505703 (2009).
- [15] G. Henkelman and H. Jónsson, *J. Chem. Phys.* **113**, 9978 (2000).
- [16] G. Henkelman, B. Uberuaga, and H. Jónsson, *J. Chem. Phys.* **113**, 9901 (2000).
- [17] T. Arai and M. Tomitori, *Appl. Surf. Sci.* **157**, 207 (2000).
- [18] K. Kobayashi, H. Yamada, T. Horiuchi, and K. Matsushige, *Appl. Surf. Sci.* **157**, 228 (2000).
- [19] M. Guggisberg, O. Pfeiffer, S. Schär, V. Barwich, M. Bammerlin, C. Loppacher, R. Bennewitz, A. Baratoff, and E. Meyer, *Appl. Phys. A: Mater. Sci. Process.* **72**, S19 (2001).
- [20] P. Rahe, R. Bechstein, J. Schütte, F. Ostendorf, and A. Kühnle, *Phys. Rev. B* **77**, 195410 (2008).
- [21] F. Loske, P. Rahe, and A. Kühnle, *Nanotechnology* **20**, 264010 (2009).
- [22] S. Molitor, P. Güthner, and T. Berghaus, *Appl. Surf. Sci.* **140**, 276 (1999).
- [23] A. Schwarz, W. Allers, U. D. Schwarz, and R. Wiesendanger, *Phys. Rev. B* **61**, 2837 (2000).
- [24] J. M. Mativetsky, S. A. Burke, R. Hoffmann, Y. Sun, and P. Grutter, *Nanotechnology* **15**, S40 (2004).
- [25] S. Koch, M. Langer, S. Kawai, E. Meyer, and T. Glatzel, *J. Phys.: Condens. Matter* **24**, 314212 (2012).
- [26] B. Such, T. Glatzel, S. Kawai, E. Meyer, R. Turanský, J. Brndiar, and I. Štich, *Nanotechnology* **23**, 045705 (2012).
- [27] M. Ondráček, C. González, and P. Jelínek, *J. Phys.: Condens. Matter* **24**, 084003 (2012).
- [28] See <http://webbook.nist.gov/chemistry>.
- [29] K. P. Huber and G. Herzberg, *Constants of Diatomic Molecules, Molecular Spectra and Molecular Structure* (Van Nostrand Reinhold Co., New York, 1979), Vol. IV, Chap. 10 .